Nat Hazards (2009) 50:479–496
DOI 10.1007/s11069-009-9355-6

ORIGINAL PAPER

Probability-weighted hazard maps for comparing different flood risk management strategies: a case study

Giuliano Di Baldassarre · Attilio Castellarin · Alberto Montanari · Armando Brath

Received: 19 October 2007 / Accepted: 19 January 2009 / Published online: 24 February 2009

Abstract The study proposes an original methodology for producing probability-weighted hazard maps based on an ensemble of numerical simulations. These maps enable one to compare different strategies for flood risk management. The methodology was applied over a 270-km^2 flood-prone area close to the left levee system of a 28-km reach of the river Reno (Northern Central Italy). This reach is characterised by the presence of a weir that allows controlled flooding of a large flood-prone area during major events. The proposed probability-weighted hazard maps can be used to evaluate how a structural measure such as the mentioned weir alters the spatial variability of flood hazard in the study area. This article shows an application by constructing two different flood hazard maps: a first one which neglects the presence of the weir using a regular levee system instead, and a second one that reflects the actual geometry with the weir. Flood hazard maps were generated by combining the results of several inundation scenarios, simulated by coupling 1D- and 2D-hydrodynamic models.

Keywords Flood hazard · River Po plan · Hydrodynamic models · Flood inundation mapping

1 Introduction

Flood inundations have the potential to cause fatalities, displacement of people, and damage to the environment, to severely compromise economic development (European Parliament, Council 2007). Flooding accounts for 40% of all the natural hazards worldwide and half of all the deaths caused by natural disasters (e.g. Ohl and Tapsell 2000; Jonkman and Vrijling 2008). In recent years, Europe suffered several major floods, from the

G. Di Baldassarre (✉)
School of Geographical Sciences, University of Bristol, University Road, Bristol BS8 1SS, UK
e-mail: g.dibaldassarre@bristol.ac.uk; giuliano.dibaldassarre@mail.ing.unibo.it

G. Di Baldassarre · A. Castellarin · A. Montanari · A. Brath
School of Civil Engineering (Dept. DISTART), University of Bologna, Bologna, Italy

widespread floods with dramatic damages in Central Europe, summer 2002, to the more recent events in England and Wales, summer 2007.

Floods are natural phenomena which cannot be prevented; nevertheless, some human activities contribute to an increase in the likelihood and adverse impacts of flood events (European Parliament, Council 2007). First, the reduction of the natural water retention by inappropriate land use and river management (e.g. continuous embankments) increases the scale and the frequency of floods. Recent analyses investigated such effects on flood hazard (see, e.g. Fohrer et al. 2001; Wooldridge et al. 2001; Brath et al. 2003; Camorani et al. 2006). Second, there has been an increasing vulnerability of flood-prone areas because of the growing number of people and economic assets located in flood risk zones (flood-prone areas are traditionally zones of special importance as they offer favourable conditions for human settlements and economic development). Finally, flood risk, that may be defined as the product of probability of flood and associated damage (i.e. the damage expectation, Merz et al. 2007), increases with economic development given that potential damage increases.

During the last two centuries, the height of levees has increased and rivers have become more and more controlled. The levee heightening, to protect the flood-prone areas, adds a component to the potential damage (Vis et al. 2003). In fact, after raising levees, people feel safer and investments in the prone area increase. Nevertheless, at the same time, with steadily increasing levee heights, the potential flood depth increases. Figure 1a reports the geometry of a river Po cross-section (located in Pontelagoscuro, approximately 80 km from the coast and just before the apex of the river Po delta) clearly showing the heightening of levees. Also, Fig. 1b shows the increase of the length of the levee system and the corresponding increase of the maximum water level during historical flood events.

Flood risk management strategies based on the construction of levees may be called resistance strategies (Vis et al. 2003). The design of levees and other water-retaining structures is usually based on an acceptable probability of overtopping and the portion of risk that remains is called residual risk (van Manen and Brinkhuis 2005). Residual flood risk behind levees is largely unaccounted. Levees are usually characterised by a uniform safety level (e.g. return period equal to 200 years). It implies that streamflows above the design discharge may cause flooding anywhere and even at several locations at the same time, and therefore the evolution of the flood event is unpredictable. It is obvious that this condition is undesirable (e.g., in case of exceptional events a large area must be evacuated as all areas adjacent to the river theoretically have the same probability of flooding).

A different approach to flood risk management is the so-called resilience strategy. The concept of resilience originates from ecology (e.g. Holling 1973) and was introduced, in the context of flood risk management, by De Bruijn and Klijn (2001). The idea behind the resilience approach is living with floods instead of fighting floods. In this approach, flooding is allowed in certain areas, whereas the impact of flooding is minimised through policies of land-use planning and management (e.g. Vis et al. 2003).

Directive 2007/60/Ec of the European Parliament (2007) states that flood risk management policies may comprise the promotion of sustainable land use practices, improvement of water retention as well as the controlled flooding of certain areas in the case of a flood event. In this context, two different flood risk management policies were compared in an Italian test site: a traditional resistance strategy, based on the use of a regular levee system, and an alternative approach, based on the use of a hydraulic structure that allows controlled flooding of certain areas, where the expected flood damage is limited.

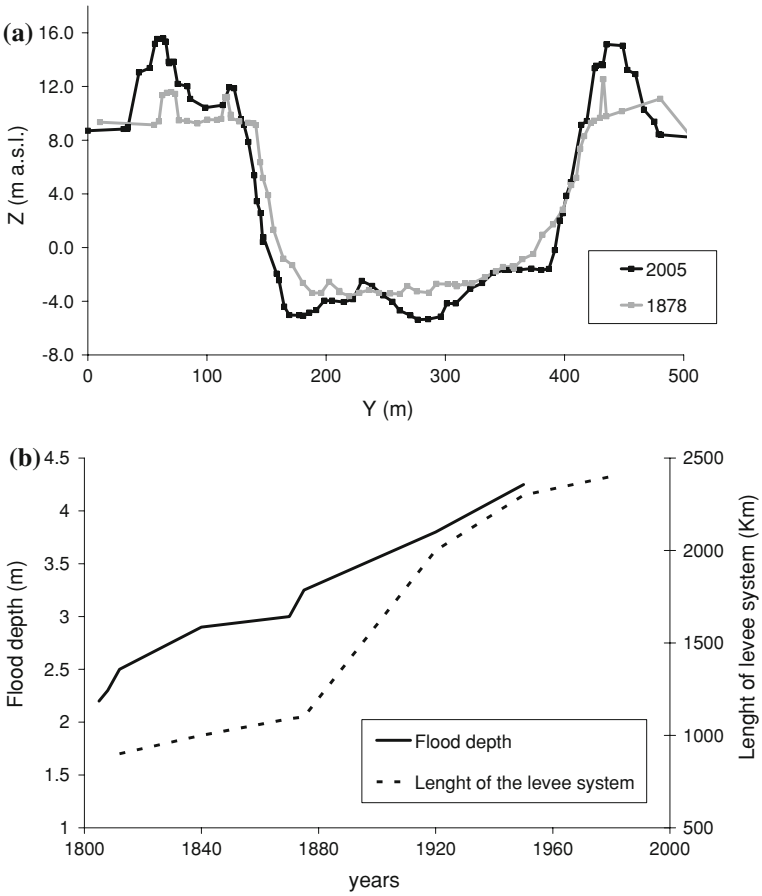

Fig. 1 River Po at Pontelagoscuro (44°53′ N 11°36′ E), Italy: **a** cross river section in 1878 and 2005; **b** evolution in time of the overall levee system length for the river Po in the last two centuries and corresponding increase of the flood depth at Pontelagoscuro (courtesy of Autorità di Bacino del fiume Po, Italy)

In order to analyse the two different strategies an innovative approach for producing probability-weighted hazard maps based on an ensemble of numerical simulations was developed: several inundation scenarios (corresponding to different levee breach locations, geometries and evolutions in time) were simulated by coupling 1D and 2D hydrodynamic models; then, results of each scenario, in terms of water depth and flow velocity, were combined in order to assess the inundation hazard. By using this procedure, two different flood hazard maps were generated: a first one that refers to a continuous levee system (characterised by a homogeneous safety level) and a second one which is associated with the presence of an existing structure that enables a controlled flooding.

Comprehensive risk analyses have to take into account the hydrological, hydraulic, economic, social and ecological aspects of the flood risk (e.g. Hall et al. 2005; Dawson et al. 2005; Merz et al. 2007). In particular, flood risk assessment requires complex deterministic models for representing the relevant processes or the use of probabilistic models (Apel et al. 2006). Given that our study aims to evaluate two different flood risk

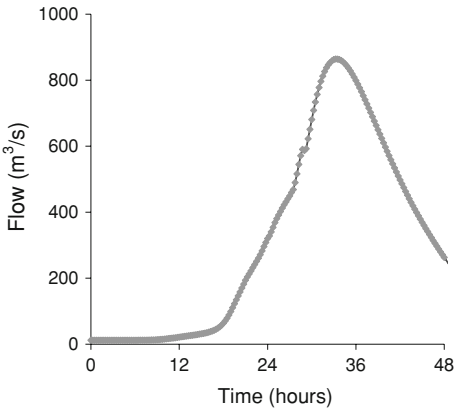

Fig. 2 Synthetic hydrograph: 100-year flood (Autorità di Bacino del Reno 1998)

policies, the analysis was limited to hydraulic modelling, levee failure processes and hazard mapping. Therefore, the impact of hydrological processes on flood hazard was not investigated in the study. This study referred instead to a synthetic hydrograph corresponding to an assigned probability of occurrence (100-year flood, Fig. 2) identified by a previous study based on statistical analysis of historical flood events (Autorità di Bacino del Reno 1998).

2 Study area

The analysis was performed on a 270-km^2 flood-prone area close to the left levee system of a 28-km reach of the river Reno, near the city of Ferrara in Northern Central Italy. The whole study area (Fig. 3) is bounded by the embankments of the state road SS 255 and the Bologna–Venezia railway, the left levees of the river Reno, and the right levees of the river Po Morto di Primaro.

The study area consists of agricultural land, residential areas ($\sim$25,000 inhabitants) and a few industrial plants. The study area was affected by two major flood events: a first one in 1949 (see Fig. 3b) that inundated an area equal to 60 km^2, and a second one in 1951 that inundated an area equal to 116 km^2. Both inundation events were caused by left levee breaches.

Over the past few decades, regulation works have changed the geometry of the river. Nevertheless, the flood risk of this area is very high: the hydraulic capacity of the reach is about 500–600 m^3 s^{-1} corresponding to a return period of about 25–50 years (Autorità di Bacino del Reno 2002); the Reno levees are about 8–11 m high and the riverbed is hanging since its altitude is higher than the flood-prone area; about 25,000 inhabitants live there and there are some industrial sites.

The topographic data available for the study are: a 10-m resolution DTM (Digital Terrain Model, Fig. 3a); a survey of the principal breaklines (levees, road embankments, railway embankments) and 35 cross-sections of the 28-km reach of the river Reno.

After the 1951 flood event, a lateral weir 100 m wide, called the Gallo weir, was constructed in the left levee of the river Reno. The Gallo weir is located approximately in the same place as the 1949 and 1951 breaches (see Fig. 3b). This hydraulic structure allows controlled flooding of a certain area, where the expected economic damage is limited. The presence of the weir alters the safety level of the flood-prone area along the river Reno,

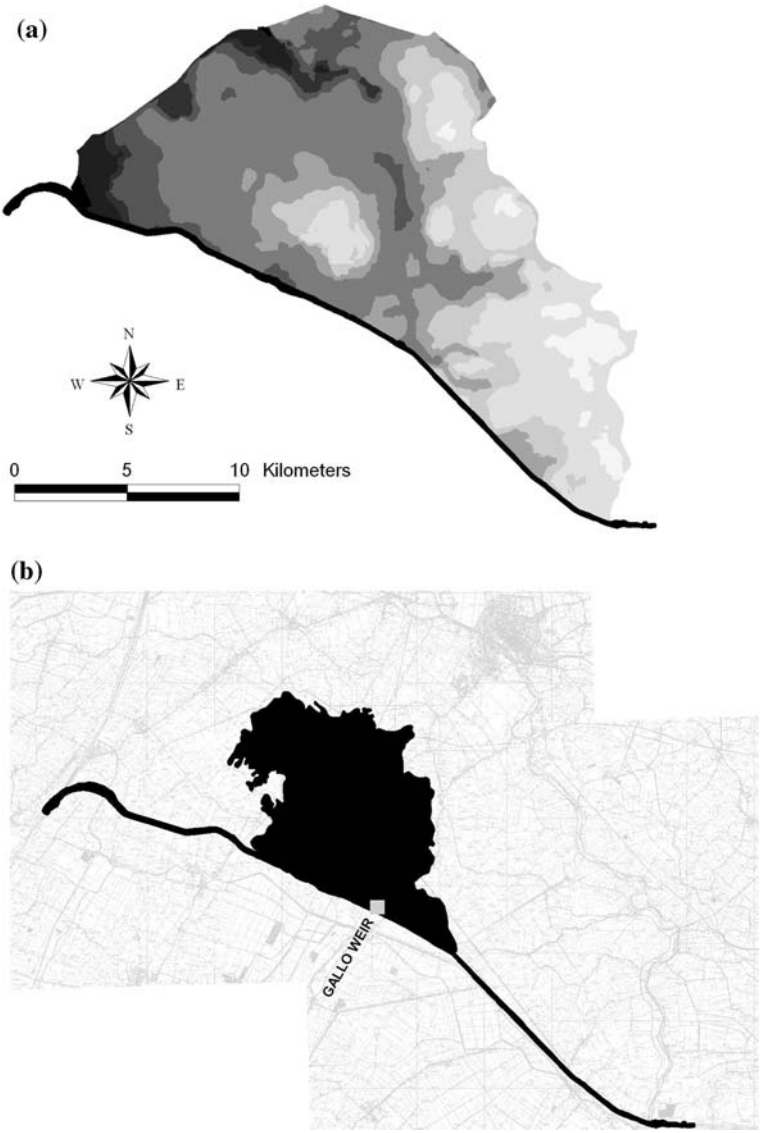

Fig. 3 Study area: **a** 28-km reach of the river Reno considered in the study (*black line*, the river flows from West to East) and 10-m resolution DTM (grey scale from 3 m a.s.l., white, to 15 m a.s.l., black); **b** inundated area during the 1949 flood event (*black area*) and location of the Gallo weir

which would be uniformly distributed if a traditional resistance policy were used. In particular, the purpose of the weir is to increase the safety levels in the downstream flood-prone areas. Obviously, at the same time, the presence of the weir decreases the safety levels in the area affected by the controlled flooding, which, notably, is not a traditional retention basin. Therefore, the Gallo weir can be considered a structural measure for implementing controlled flooding in certain areas (European Parliament 2007). This flood risk management technique consists of allowing controlled inundation in areas where the

impact of flood can then be minimised by ad-hoc non-structural measures, such as land-use management policies, in order to minimise the consequences of flooding.

The effects of the Gallo weir on the flood inundation hazard of the entire study area have not been investigated (Autorità di Bacino del Reno 2002). In fact, at this test site the current flood risk management plan (Autorità di Bacino del Reno 2002) identifies the potentially flooded area as a buffered area of a 300-m width outside the left and right levees. This study proposes a methodology based on an ensemble of numerical simulations to produce probability-weighted hazard maps and, therefore, investigates the effects of the weir on the flood inundation hazard of the entire study area.

3 Numerical modelling of inundation scenarios

In order to simulate several inundation scenarios for generating flood hazard maps, a compromise between physical realism and computational efficiency of the model is to be defined. Therefore, numerical simulations were performed by using a hybrid methodology: flows through the lateral weir and simulated breaches were computed by a 1D approach and then adopted as the inflow boundary condition for a 2D model of the flood-prone area. In this way, dynamic flooding can be simulated whilst avoiding the onerous description of the riverbed geometry in two dimensions and, consequently, achieving a reduction in the computational time (see, e.g. Aureli et al. 2006). In particular, the study used the 1D code HEC-RAS (US Army Corps of Engineers, Hydrologic Engineering Center 2001), for simulating the hydraulic behaviour of the 28-km reach of river Reno in the presence of levee breaches and with or without the Gallo weir, and the 2D code TELEMAC-2D (Galland et al. 1991) for the floodplain flow.

3.1 One-dimensional model

HEC-RAS (US Army Corps of Engineers, Hydrologic Engineering Center 2001) solves the well-known De Saint Venant equations for unsteady open channel flow through the UNET code (Barkau 1997). Specifically, it solves the continuity equation:

$$\frac{\partial A}{\partial t} + \frac{\partial \phi Q}{\partial x_c} + \frac{\partial (1-\phi) Q}{\partial x_f} = 0 \tag{1}$$

and the momentum equation:

$$\frac{\partial Q}{\partial t} + \frac{\partial}{\partial x_c}\left(\frac{\phi^2 Q^2}{A_c}\right) + \frac{\partial}{\partial x_f}\left(\frac{(1-\phi)^2 Q^2}{A_f}\right) + gA_c\left(\frac{\partial z}{\partial x_c} + S_c\right) + gA_f\left(\frac{\partial z}{\partial x_f} + S_f\right) = 0 \tag{2}$$

with:

$$\phi = \frac{K_c}{K_c + K_f},\ K = \frac{A^{5/3}}{nP^{2/3}},\ S_c = \frac{\phi^2 Q^2 n_c^2}{R_c^{4/3} A_c^2},\ S_f = \frac{\phi^2 Q^2 n_f^2}{R_f^{4/3} A_f^2} \tag{3}$$

where Q is the total flow down the reach, A (A_c, A_f) the cross sectional area of the flow (in channel, floodplain), x_c and x_f are the distances along the channel and floodplain (these may differ between cross sections to allow for channel sinuosity), P the wetted perimeter, R the hydraulic radius (A/P), n the Manning's roughness coefficient and S the friction slope. ϕ determines how flow is partitioned between the floodplain and channel, according to the conveyances K_c and K_f. Equations 1 and 2 are discretised using the finite difference

method and solved using a four-point implicit method (box scheme, Priessmann, 1961). Levee overtopping and breaching can be analysed within HEC-RAS by modelling the levee as a lateral structure (Barkau 1997).

3.2 Two-dimensional model

2D-shallow water codes aim to solve the shallow water (or depth averaged) equations:

$$\frac{\partial h}{\partial t} + \nabla \cdot (\mathbf{u}h) = 0, \tag{4}$$

$$\frac{\partial \mathbf{u}}{\partial t} + (\mathbf{u} \cdot \nabla)\mathbf{u} + g\nabla(h + z) - \frac{v_t}{h}\nabla(h\nabla \cdot \mathbf{u}) + \frac{gn^2|\mathbf{u}|\mathbf{u}}{h^{4/3}} = 0, \tag{5}$$

where h is the flow depth, $\mathbf{u} = [u, v]$ is a 2D depth averaged flow velocity vector, z the bed elevation, g the acceleration due to gravity, n Manning's coefficient of roughness, and v_t a turbulent eddy viscosity which parameterises horizontal turbulent momentum transfer.

Solution of the Eqs. 4 and 5 was performed by using the 2D-finite element model TELEMAC-2D (Galland et al. 1991; Hervouet and Van Haren 1996). TELEMAC-2D is able to represent complex floodplain topography, dynamic wetting and drying of the floodplain and prediction of mass fluxes between channel and floodplain (Horritt et al. 2007). One of the advantages of finite element models is that they are based on an unstructured mesh that can be used for better describing the topographic discontinuities that interfere with the inundation process such as levees, road and railway embankments (Brath and Di Baldassarre 2006).

3.3 Implementation of the models

As mentioned above, a series of inundation scenarios were simulated by adopting a hybrid approach: a 1D model (HEC-RAS) in the river for computing the outflow leaving through the breach and a 2D model (TELEMAC-2D) for describing the inundation in the flood-prone area. Given that the Reno levees are 8–11 m high (Sect. 2), it can be reasonably assumed that there are no interactions between the two models (e.g. Aureli et al. 2006). Therefore, the two models were run separately: the output of the 1D model was used as the input of the 2D model. The validity of this assumption was then verified for each run by analysing the evolution in time of the water levels simulated by the 2D model in the proximity of the breach (see below, Sect. 4).

The geometry of the 28-km reach of the river Reno was described by means of 35 cross-sections and a synthetic flow hydrograph (Fig. 2) was used as upstream boundary condition while a rating curve defined the downstream boundary condition. The 1D model was calibrated by using hydrometric data (for a total of 120 points) referred to recent flood events (September 1994 and November 2000; see, Autorità di Bacino del Reno 2002).

The 2D model was used to simulate overland flow in the 270-km^2 flood-prone area. After an extensive sensitivity analysis for identifying the optimal resolution, the computational mesh was characterised by 9,437 elements and 4,885 nodes (the cell size varies from 10 to 500 m). The altimetry was determined by means of the 10-m resolution DTM (Fig. 3a) and a survey of the principal breaklines (e.g. road embankment). The Manning's coefficients of the flood-prone area were selected to represent the physical characteristics of the flood-prone area according to standard tables (e.g., Chow 1959) and sensitivity

analysis of the 2D model previously performed in similar test sites (e.g. Horritt et al. 2007). Then, in order to have an indication on the reliability of the model, the 2D model was tested by simulating the 1949 flood event. The agreement between the historical flood extent map (Fig. 3b) and the model simulation was evaluated by the standard performance index (e.g. Bates 2004) and resulted equal to 85%.

4 Numerical simulations

Numerical simulations were performed in order to generate two flood hazard maps: a first one which neglects the presence of the Gallo weir, using a regular levee system instead, and a second one that reflects the actual geometry with the presence of the Gallo weir that allows the controlled flooding of an area where the expected flood damage is limited.

In order to generate flood hazard maps, several inundation scenarios, representing the absence of the Gallo weir (hypothetical scenario, Sect. 4.1) or its presence (scenario representative of the current situation, Sect. 4.2), were simulated as described below. Ensemble simulations were used in order to inspect the approximation induced by (i) positioning the breach in different locations of the left levee and (ii) assuming different hypotheses of breach development. In this way, it is possible to evaluate the uncertainty induced by the above unknown information. The study is affected by other uncertainties induced by imprecise input data (hydrological input, river and floodplain geometry), model structural uncertainty and model parameters (e.g. Montanari 2005). These other sources of uncertainty were neglected by assuming that these affect the scenarios considered in a similar fashion and therefore that the results of our comparison are still suitable in the more general case.

4.1 Resistance strategy: hypothetical scenario

The hypothetical scenario neglects the presence of the Gallo weir, using a regular levee system instead (resistance strategy). As mentioned above, with the traditional resistance approach all the areas theoretically have the same probability of flooding.

In order to evaluate where levees might be overtopped, a 1D preliminary simulation was carried out. In particular, the 1D model was used for simulating a synthetic flood event corresponding to return period of 100 years (Autorità di Bacino del Reno 1998). In order to evaluate where levees may be overtopped and breached, during this preliminary 1D simulation flooding is restricted to the area inside the embankments (i.e. no overflow is allowed). As Fig. 4a shows, the preliminary 1D simulation points out that the left levee system is not able to contain the 100-year flood. It means that the left levee may be overtopped anywhere along the considered reach. Given that one can not establish the exact location where the overtopping will start, 30 equispaced potential locations for breaches along the river Reno were identified (Fig. 4b). Also, according to the description of the historical levee breaches (Govi and Turitto 2000), the presence of only one breach along the levee system under study was assumed.

An ensemble simulation was then performed in order to account for the uncertainty associated with the location and evolution of the breach. Accordingly, for each possible location different geometries of the levee failure were considered. For each breach location, this study considered different characteristics of the levee overtopping and

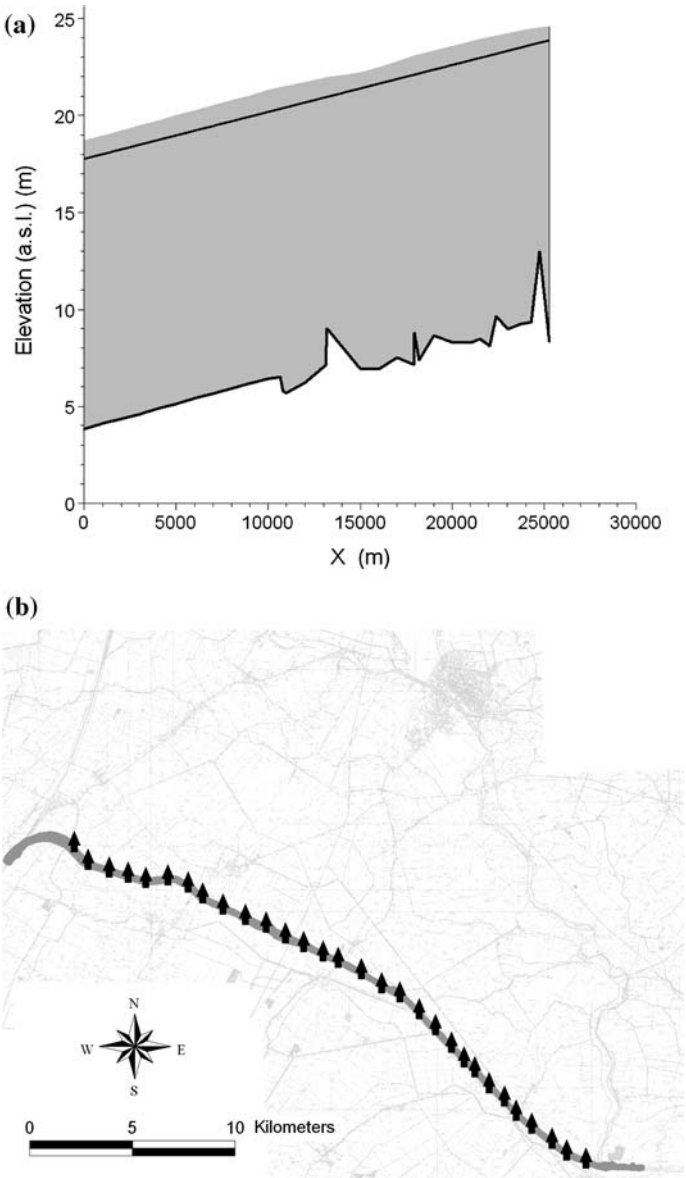

Fig. 4 Absence of Gallo weir (resistance strategy): **a** results of the preliminary 1D simulation in terms of maximum water depth (*grey*) and left levee elevation (*upper black line*), the lower black line represents the bed elevation; **b** location of possible levee breach (*black arrows*) along the river Reno (*grey line*)

breaching in terms of time of formation (overall duration of the breach development, T), width of the breach (W), and depth of the breach (D). The breach was assumed to start when the levee is overtopped. Given that it is impossible to determine a priori the value of T, W and D, a random generation of 200 different combinations of T, W and D was carried out under the assumption of uniform distribution of the three parameters

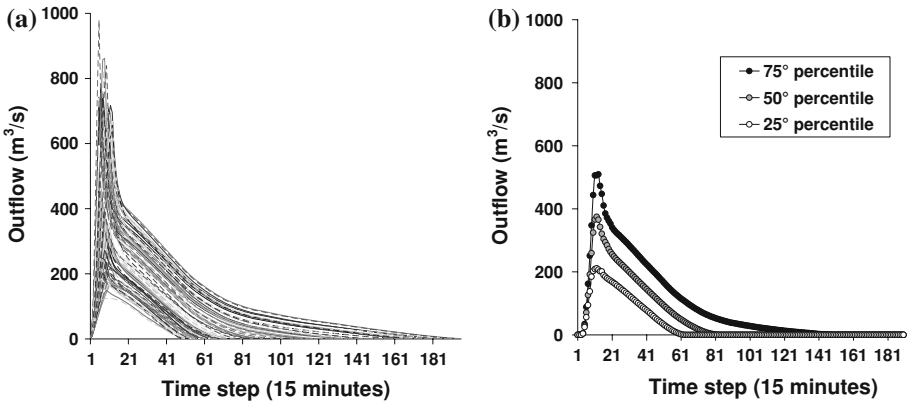

Fig. 5 Levee breach: **a** outflows obtained by means of 1D simulations for a particular location of the breach; **b** three representative hydrographs used as inflow in the 2D model

and $1\text{ h} < T < 3\text{ h}$; $100\text{ m} < W < 300\text{ m}$; $0.5\text{ m} < D < 4\text{ m}$ (floodplain plan); according to historical data available for neighbouring sites (river Po, Govi and Turitto 2000). Then, for each breach location, 200 1D simulations (each characterised by different T, W and D) were carried out by using the 100-year hydrograph as upstream boundary condition. In total 200 breach outflows hydrographs were generated (Fig. 5a). A distribution of hydrographs enables one to assess the uncertainty associated with the location and the evolution of the breach. In order to limit the number of 2D simulations, these outflows were statistically summarised by defining reference hydrographs for each breach location: High (H); Medium (M); Low (L), corresponding to, the 75th percentile, the 50th percentile and the 25th percentile, respectively. A sensitivity analysis showed that the three reference hydrographs do not change significantly with a number of simulations larger than 100–150. These reference hydrographs (Fig. 5b) were then used as the inflow condition for the 2D model to simulate inundation scenarios. The study used the 25th and 75th percentiles (instead of, for example, the 5th and 95th percentiles) in order to obtain plausible reference hydrographs and omit unlikely (i.e., extreme) combinations of the variables considered, which may originate as a result of the uniform distribution that is used to represent the frequency of the variables. Therefore, if for example, the 5th and 95th percentiles were used unrepresentative hydrographs would be obtained. In total, in the case of the absence of the Gallo weir (resistance strategy), 6000 1D unsteady flow simulations (30 different breach locations multiplied by 200 different breach characteristics) were performed and 90 2D unsteady flow simulations for the overland flow (30 different breach locations multiplied by three representative inflow hydrographs).

As an example, Fig. 6 shows the results in terms of maximum water depth for some different inundation scenarios (e.g. simulation (4, H), where 4 is the location of the breach and H is the inflow hydrograph, etc.). One can observe the different locations of the breach (Fig. 6). Also, it is interesting to note that the simulated water depths in the flood-prone areas are lower than 3 m. Given that the Reno levees are 8–11 m high (Sect. 2), the results of the 2D models pointed out that the assumption of no interactions between the two models is reasonable (see above, Sect. 3).

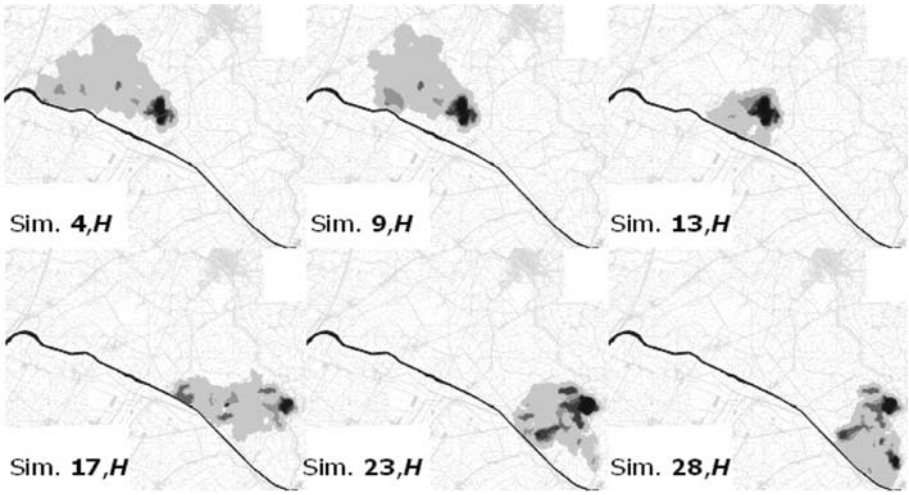

Fig. 6 Absence of the Gallo weir: example of different scenarios, results in terms of maximum water depth (grey scale, from 0 m, white, to 3 m, black)

4.2 Controlled flooding strategy: current situation scenario

The current situation scenario reflects the actual geometry with the presence of the Gallo weir that allows controlled flooding of a certain prone area (controlled flooding strategy).

As mentioned above (Sect. 4.1), without the Gallo weir, the preliminary 1D simulation indicated that left levees were not able to contain the 100-year flood (Fig. 4a). If the Gallo weir is included within the model (as a lateral structure), an analogous preliminary 1D simulation shows the effects of the Gallo structure on the hydraulic profile: because of the controlled flooding through the lateral weir, the levee system is able to contain the 100-year flood downstream of the Gallo weir and for a short portion of the river upstream of the Gallo weir (Fig. 7a). It means that the left levee may be overtopped at any point along the upstream part of the 28-km reach of the river Reno here considered, for a reach of around 9 km length (Fig. 7a). As mentioned above, one can not establish the exact location where the overtopping will start. Therefore, 10 equispaced potential locations for breaches along the upstream part of the 28-km reach of the river Reno were identified (Fig. 7b). Here, because of the presence of the Gallo weir, the inundation scenarios are characterised by a first inflow due to levee overtopping and breach, and a second inflow due to the controlled flooding through the Gallo weir (when present, see below).

This study followed a procedure analogous to the procedure adopted for the resistance strategy in the absence of Gallo weir (Sect. 4.1). In brief, in the presence of the Gallo weir, 2000 1D unsteady flow simulations (10 different breach locations times 200 different breaches) and 30 2D unsteady flow simulations for the overland flow (10 different breach locations multiplied by 3 representative inflow hydrographs) were performed.

Figure 8 shows some results in terms of maximum water depth (in metres) for some different inundation scenarios. One can observe that, on the one hand, medium (M), or low (L), flows through the levee breach, flooding occurs both through the breach and the Gallo weir; on the other hand, high (H) flows through the levee breach, no flow occurs through the Gallo weir because of the high quantity of water flooding through the breach (see e.g. Fig. 8).

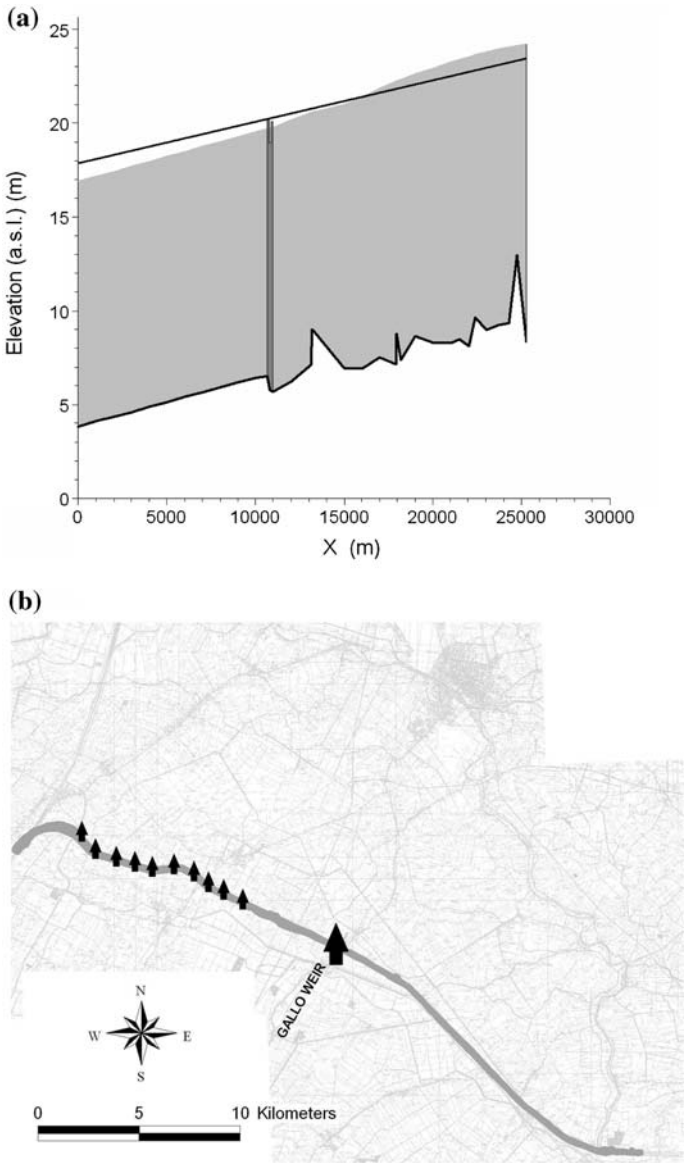

Fig. 7 Presence of the Gallo weir: **a** results of the preliminary 1D simulation in terms of maximum water depth (*grey*) and left levee elevation (*upper black line*), the lower black line represents the bed elevation; **b** location of possible levee breach (*black short arrows*) and of the Gallo controlled flooding (*black long arrow*)

5 Flood hazard map

In order to generate a flood hazard map, results of the 2D simulations, in the absence or presence of the Gallo weir, were combined by evaluating the expected water depth (WD_i) and the expected scalar velocity (SV_i), for each computational node i of the study area:

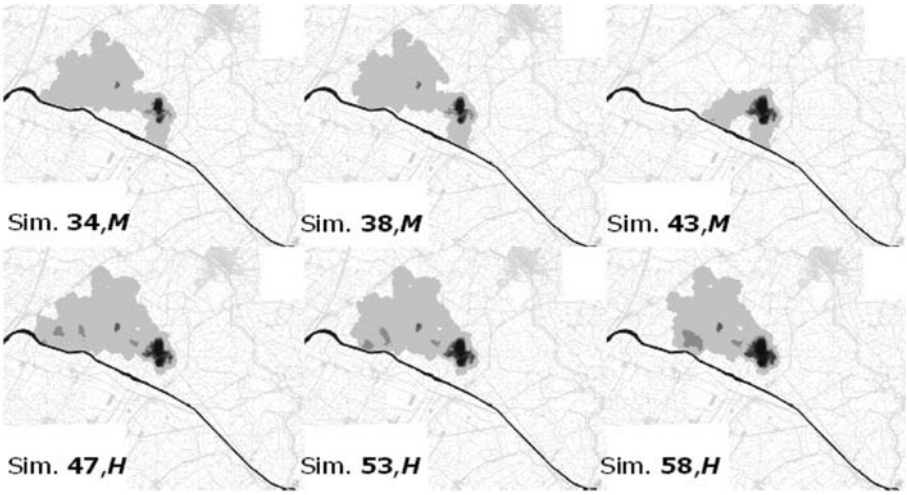

Fig. 8 Presence of the Gallo weir: example of different scenarios, results in terms of maximum water depth (grey scale, from 0 m, white, to 3 m, black)

$$WD_i = \sum_{j=1}^{NS} x_j WD_{i,j}, \tag{6}$$

$$SV_i = \sum_{j=1}^{NS} x_j SV_{i,j}, \tag{7}$$

where NS is the number of 2D-simulations. $WD_{i,j}$ and $SV_{i,j}$ are the maximum water depth and the maximum scalar velocity at the node i for the simulation j, and x_j is the weight of the simulation j obtained as a function of the probability of occurrence of the simulation itself, depending on the location and the magnitude of the breach:

$$x_j = wl_j wp_j \tag{8}$$

where wl_j depends on the location of the breach and is linearly proportional to the difference between the maximum simulated water elevation and the levee system elevation (see Figs. 4a, 7a): the more is this difference the higher is the possibility that the breach occurs (i.e. the levee system is more likely to be not able to contain the flood); wp_j depends on the magnitude of the breach and it is equal to 0.25 for low (L) or high (H) flows through the levee breach and it is equal to 0.50 for medium (M) flow. This choice was made to give the same weight to medium and high or low flows. As a result, expected values of water depth and scalar velocity are obtained in view of the uncertainties due to the unknown position and development of the levee breach.

The scientific literature proposes several water depth–velocity hazard curves (e.g. ACER Technical Memorandum No. 11 1988; Vrisou van Eck and Kok 2001; Penning-Rowsell and Fordham 1994; Staatscourant 1998). Despite these efforts, quantifying the expected flood damage is very difficult: the impact of a flood event on a prone area is related to several other factors such as the education of the population, the time of the day, and the day of the week when the inundation occurs; also, the consequences of a flood can last several months. For these reasons a flood hazard map was generated in order to

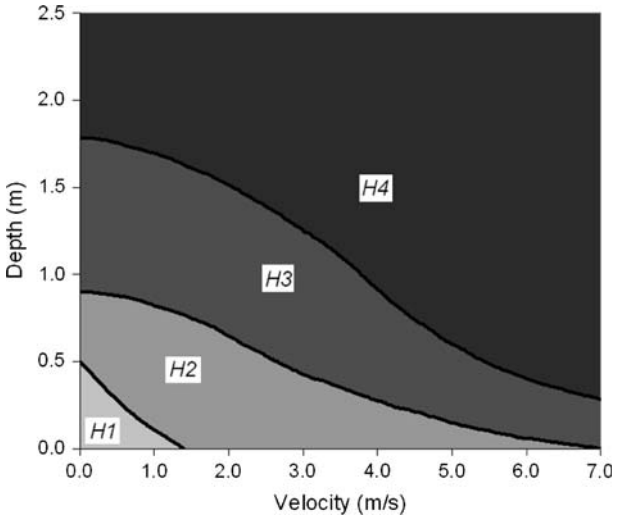

Fig. 9 Flood depth–velocity hazard classification herein utilised

evaluate the effects of the presence of the Gallo weir on the safety level of the flood-prone area. The study aimed at evaluating how the spatial distribution of hazard in the test site is affected by the presence of the Gallo weir; therefore it does not take into account other possible factors (e.g., land-use). Figure 9 shows a possible relationship between flood depth, velocity and hazard. The curve represented in Fig. 9 is analogous to that described in the ACER Technical Memorandum No. 11 (1988). This relationship is appropriate for the test site under study as it was derived for permanent residences, commercial and public buildings, and worksite areas (ACER Technical Memorandum No. 11 1988). Rigorously, the hazard level is to be evaluated by combining flood depth and velocity for each simulation at each time step. In order to make the procedure faster, the value of the expected water depth and the expected scalar velocity were used for classifying the flood-prone area in five hazard classes: from H0, low flood hazard (corresponding to the area not concerned by inundation scenarios), to H4, very high flood hazard (see Fig. 9). In this way, a first flood hazard map was generated combining the results of inundation scenarios corresponding to the hypothesis of regular levee system (Fig. 10a) and a second flood hazard map, combining the results of the inundation scenarios corresponding to the presence of the Gallo weir (Fig. 10b). The two flood hazard maps obtained by applying the simplified procedure are conservative. In fact, the proposed methodology tends to overestimate the hazard level as the timing of the maximum water depth is generally different from the timing of the maximum scalar velocity.

While common sense and standard methodologies (Autorità di Bacino del Reno 2002) did not enable the evaluation of the effects of the weir on the flood inundation hazard of the entire study area (Sect. 2), the proposed methodology enabled the investigation of such effects. Specifically, by analysing the two flood hazard maps in Fig. 10 one can observe that under the hypothesis of a regular levee system, inundation hazard is distributed over a very large area (e.g. resistance strategy, Sect. 1), while with the Gallo weir, flood hazard is more localised (Fig. 10b). In particular, with the presence of the Gallo weir, hazard is increased in the depressed area (see also DTM, Fig. 3a), where hazard was already high with a regular levee system (Fig. 10a). Therefore, the numerical analysis allowed the

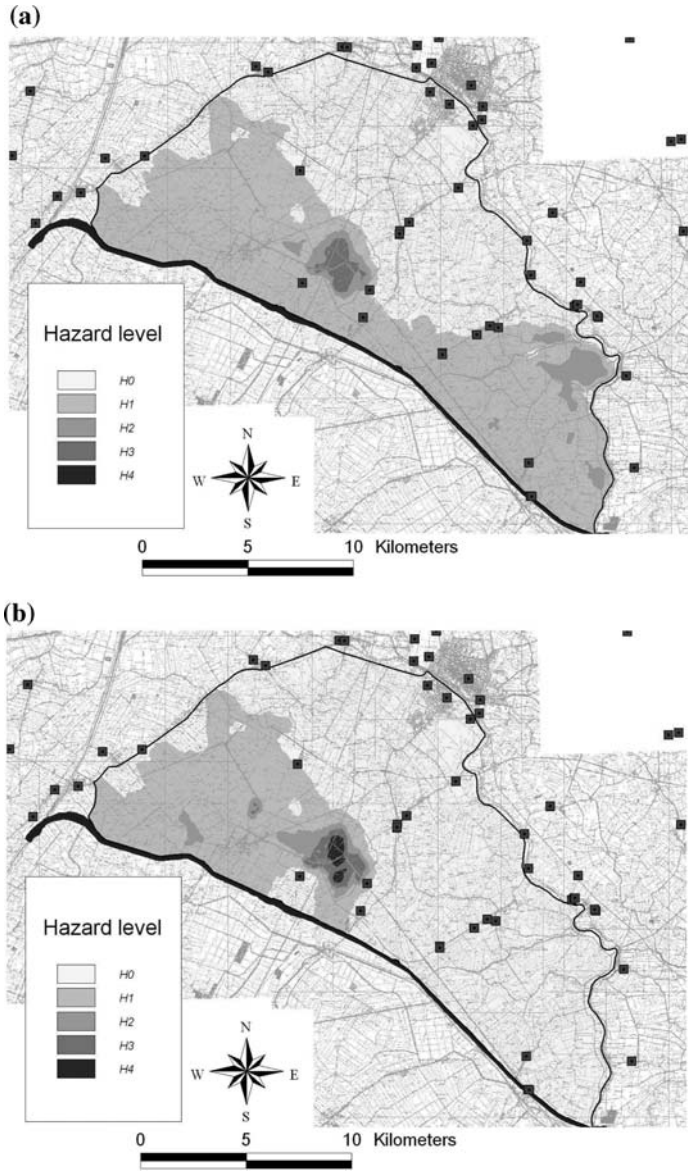

Fig. 10 Flood hazard maps: **a** absence of the Gallo weir; **b** presence of the Gallo weir; location of industrial plants (*square dots*)

assessment of the effect of the hydraulic structure considered herein: due to controlled flooding, hazard slightly increases where it was already high and decreases significantly in a large part of the study area. This change should be regarded as an improvement since, for example, without the Gallo weir, many industrial plants and storages (see locations in Fig. 10) would be located in H1 or H2 hazard zones; with the hydraulic structure they are all located in a H0 hazard zone. Given that, as mentioned above, the proposed methodology provides conservative flood hazard maps, an additional comparison of the two flood

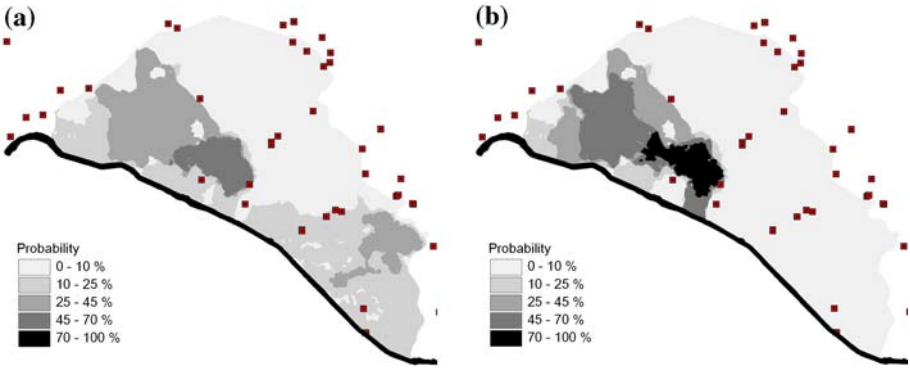

Fig. 11 Probability-of-inundation maps: **a** absence of the Gallo weir; **b** presence of the Gallo weir; location of industrial plants (*square dots*)

risk management strategies was carried out. The results of the inundation scenarios were reclassified in order to generate binary wet/dry maps of the total flood extent. Then a first probability-of-inundation map (e.g. Aronica et al. 2002) was produced by combining the binary maps corresponding to the hypothesis of regular levee system (Fig. 11a) and a second probability-of-inundation map, that combines the results of the inundation scenarios corresponding to the presence of Gallo weir (Fig. 11b). Specifically, the probability-of-inundation map represents the percentage of scenarios in which each point of the test site is classified as inundated. The analysis of Fig. 11 is similar to that of Fig. 10. The findings of this study may help planning future urban development and location of industrial sites in this important flat area.

The methodology proposed may be used to compare different strategies for flood risk mitigation and management. For instance, the river Po Authority (Autorità di Bacino del fiume Po, Italy) is currently evaluating the opportunity to implement innovative procedures of controlled flooding of certain areas, instead of continuous levee heightening. Specifically, with the current geometry (e.g. Fig. 1), given that the levee system is designed for a 200-year flood, disastrous consequences are likely to occur in case of levee failures during higher magnitude events. The proposed methodology can be applied to compare two alternative flood risk management policies: a first one based on continuous levee heightening and a second one based on the implementation of controlled flooding techniques.

6 Conclusion

The study aimed at evaluating the effects of a controlled flooding on the inundation hazard of a flood prone area using a specific case study in Italy. The analysis was performed by generating two different flood hazard maps: one which neglects the presence of a lateral weir, using a regular levee system instead, and one that reflects the actual geometry with the presence of a lateral weir that allows controlled flooding. In particular, 1D and 2D flood inundation models were utilised and an innovative methodology for producing probability-weighted hazard maps based on ensembles of numerical simulations was developed. The use of ensemble simulations allowed one to account for relevant sources of uncertainties for assessing flood hazard.

The results pointed out that controlled flooding of large flood-prone areas—where damage is minimised by adopting ad-hoc non-structural measures—may be effective for flood risk mitigation and management. The study pointed out that hazard increases slightly where it was already high with a regular levee system and decreases significantly in a large part of the study area; this change should be regarded as an improvement, especially when considering the location of industrial plants and storages. The results of the study are unavoidably associated with the considered test site. Nevertheless, the proposed methodology for producing probability-weighted hazard maps based on ensembles of numerical simulations could be a useful tool for comparing different strategies for flood risk mitigation and management.

Acknowledgements The authors are extremely grateful to the Autorità di Bacino del Reno, Settore Tecnico e Protezione Civile and Consorzio Generale di Bonifica nella Provincia di Ferrara allowing access to their data of river Reno. The authors wish to thank Jeff Neal and Guy Schumann for their valuable suggestions and comments. Three unknown Reviewers and the Associate Editor are acknowledged for their useful and constructive reviews.

References

ACER Technical Memorandum No. 11 (1988) Assistant Commissioner—Engineering and Research, Downstream Hazard Classification Guidelines, Denver, Colorado, U.S. Department of the Interior, Bureau of Reclamation

Apel H, Thieken AH, Merz B, Bloschl G (2006) A probabilistic modelling system for assessing flood risks. Nat Hazards 38:79–100. doi:10.1007/s11069-005-8603-7

Aronica G, Bates PD, Horritt MS (2002) Assessing the uncertainty in distributed model predictions using observed binary pattern information within GLUE. Hydrol Process 16(10):2001–2016. doi:10.1002/hyp.398

Aureli F, Mignosa P, Ziveri C, Maranzoni A (2006) Fully-2D and quasi-2D modelling of flooding scenarios due to embankment failure, River Flow 2006, Taylor & Francis Group, London. ISBN: 0-415-40815-6

Autorità di Bacino del Reno (1998) Generazione di idrogrammi di piena nel bacino del fiume Reno chiuso a Casalecchio (in Italian). Published online on http://www.regione.emilia-romagna.it/bacinoreno, Bologna

Autorità di Bacino del Reno (2002) Piano Stralcio per l'Assetto Idrogeologico (in Italian). Published online on http://www.regione.emilia-romagna.it/bacinoreno, Bologna

Barkau RL (1997) UNET One dimensional unsteady flow through a full network of open channels user's manual. US Army Corps of Engineerings, Hydrologic Engineering Center, Davis

Bates PD (2004) Computationally efficient modelling of flood inundation extent. European Science Foundation Workshop, Ed. BIOS, Bologna

Brath A, Di Baldassarre G (2006) Modelli matematici per l'analisi della sicurezza idraulica del territorio. L'Acqua 6:39–48. ISSN: 1125–1255

Brath A, Montanari A, Moretti G (2003) Assessing the effects on flood risk of land-use changes in the last five decades: an Italian case study. IAHS Publication no. 278, IAHS Press, UK

Camorani G, Castellarin A, Brath A (2006) Effects of land-use changes on the hydrologic response of reclamation systems. Phys Chem Earth 30:561–574

Dawson RJ, Hall JW, Sayers PB, Bates PD, Rosu C (2005) Sampling-based flood risk analysis for fluvial dike systems. Stoch Environ Res Risk Anal 19(6):388–402. doi:10.1007/s00477-005-0010-9

De Bruijn KM, Klijn F (2001) Resilient flood risk management strategies. In: Guifen L, Wenxue L (eds) Proceedings of the IAHR congress, September 16–21, 2001, Beijing China. Tsinghua University Press, Beijing, ISBN: 7-302-04676-X/TV, pp 450–457

European Parliament Council (2007) Directive 2007/60/Ec of the European Parliament and of the council of 23 October 2007 on the assessment and management of flood risks. http://eur-lex.europa.eu/en/index.htm

Fohrer N, Haverkamp S, Eckhardt K, Frede H-G (2001) Hydrologic response to land use changes on the catchment scale. Phys Chem Earth 26:577–582

Galland JC, Goutal N, Hervouet JM (1991) TELEMAC: a new numerical model for solving shallow water equations. Adv Water Resour 14(3):138–148. doi:10.1016/0309-1708(91)90006-A

Govi M, Turitto O (2000) Casistica storica sui processi d'iterazione delle correnti di piena del Po con arginature e con elementi morfotopografici del territorio adiacente (in Italian), Istituto Lombardo Accademia di Scienza e Lettere

Hall JW, Sayers PB, Dawson RJ (2005) National-scale assessment of current and future flood risk in England and Wales. Nat Hazards 36:147–164. doi:10.1007/s11069-004-4546-7

Hervouet JM, Van Haren L (1996) Recent advances in numerical methods for fluid flows. In: Anderson MG, Walling DE, Bates PD (eds) Floodplain processes. Wiley, Chichester, UK, pp 183–214

Holling CS (1973) Resilience and stability of ecological systems. Annu Rev Ecol Syst 4:1–24. doi:10.1146/annurev.es.04.110173.000245

Horritt MS, Di Baldassarre G, Bates PD, Brath A (2007) Comparing the performance of 2-D finite element and finite volume models of floodplain inundation using airborne SAR imagery. Hydrol Process 21:2745–2759. doi:10.1002/hyp.6486

Hydrologic Engineering Center (2001) Hydraulic reference manual. U.S. Army Corps of Engineers, Davis, USA

Jonkman SN, Vrijling JK (2008) Loss of life due to floods. J Flood Risk Manag 1(1):43–56. doi:10.1111/j.1753-318X.2008.00006.x

Merz B, Thieken AH, Gocht M (2007) Flood risk mapping at the local scale: concepts and challenges. In: Begum S, Stive MJF, Hall JW (eds) Flood risk management in Europe: innovation in policy and practice. Series: Advances in natural and technological hazards research, vol 25. Springer, Dordrecht, Chapter 13, p 231–251

Montanari A (2005) Large sample behaviors of the generalized likelihood uncertainty estimation (GLUE) in assessing the uncertainty of rainfall-runoff simulations. Water Resour Res 41:W08406. doi:10.1029/2004WR003826

Ohl C, Tapsell S (2000) Flooding and human health: the dangers posed are not always obvious. BMJ 321:1167–1168. doi:10.1136/bmj.321.7270.1167

Penning-Rowsell E, Fordham M (1994) Floods across Europe. Hazard assessment, modelling and management. Middlesex University Press, Middlesex. ISBN: 1 898253 01 3

Staatscourant (1998) Regeling oogstschade (1998) Staatscourant 1998, no. 244. Ministerie van Algemene Zaken, Den Haag, pp 16–17

Stuart-Menteth A (2007) RMS releases report on the summer 2007, U.K. Floods. http://www.rms.com

van Manen SE, Brinkhuis M (2005) Quantitative flood risk assessment for Polders. Reliab Eng Syst Saf 90:229–237. doi:10.1016/j.ress.2004.10.002

Vis M, Klijn F, De Bruijn KM, Van Buuren M (2003) Resilience strategies for flood risk management in the Netherlands. Int J River Basin Manag 1(1):33–44

Vrisou van Eck N, Kok M (2001) Standaardmethode Schade en Slachtoffers als gevolg van overstromingen. Dienst Weg-en Waterbouwkunde. Ministerie van Rijkswaterstaat, The Netherlands. Publicatie-no. W-DWW-2001-028

Wooldridge S, Kalma J, Kuczera G (2001) Parameterisation of a simple semi-distributed model for assessing the impact of landuse on hydrologic response. J Hydrol (Amst) 254:16–32. doi:10.1016/S0022-1694(01)00489-9